Global parton distributions with nuclear and finite-Q^{2} corrections

J. F. Owens, A. Accardi, and W. Melnitchouk

Phys. Rev. D **87**, 094012 — Published 10 May 2013

DOI: 10.1103/PhysRevD.87.094012

JLAB-THY-13-5

Global parton distributions with nuclear and finite-Q^2 corrections

J.F. Owens[1], A. Accardi[2,3], W. Melnitchouk[3]

[1]*Florida State University, Tallahassee, Florida 32306-4350*

[2]*Hampton University, Hampton, Virginia 23668*

[3]*Jefferson Lab, Newport News, Virginia 23606*

Abstract

We present three new sets of next-to-leading order parton distribution functions (PDFs) determined by global fits to a wide variety of data for hard scattering processes. The analysis includes target mass and higher twist corrections needed for the description of deep inelastic scattering data at large x and low Q^2, and nuclear corrections for deuterium targets. The PDF sets correspond to three different models for the nuclear effects, and provide a more realistic uncertainty range for the d quark PDF, in particular, compared with previous fits. We describe the PDF error sets for each choice of the nuclear corrections, and provide a user interface for utilizing the distributions.

I. INTRODUCTION

Parton distribution functions (PDFs) are necessary ingredients for any calculation of a hard scattering process involving hadrons in the initial state. Deeply-inelastic lepton-hadron scattering (DIS) experiments provide data which yield information on PDFs over a wide range of parton light-cone momentum fraction x and four-momentum transfer squared Q^2. Traditional global fits focus on the extraction of the leading twist PDFs, utilizing cuts on Q^2 and the hadronic final state mass squared $W^2 = M^2 + Q^2(1-x)/x$, where M is the nucleon mass. These cuts, which typically are of the order $Q^2 \gtrsim 4$ GeV^2 and $W^2 \gtrsim 14$ GeV^2, are designed to eliminate regions where effects that do not scale with Q^2 may be important. At any finite value of Q^2, the available range in x is therefore kinematically limited by $x < x_{\rm max} = Q^2/(W^2 - M^2 + Q^2)$. Available DIS data sets have few points above $x \approx 0.7$ when these types of cuts are applied. Other types of data such as lepton pair production or high-p_T jet production are also generally limited to regions which are sensitive to PDF momentum fraction values $x \lesssim 0.7$, or have limited statistics. There are few constraints, therefore, on the large-x behavior of PDFs, and the results of global fits using these cuts should be considered as extrapolations when evaluated above this value of x.

Aside from the intrinsic interest in the behavior of PDFs at large values of x [1–5], there are also important practical aspects to consider. The production of a state of mass m at rapidity y in proton-proton collisions at a center-of-mass energy $\sqrt{s}$ requires knowledge of PDFs at $x \approx (m/\sqrt{s})\, e^{\pm y}$ at a scale of order m. High mass states produced in the forward scattering region at large positive values of y therefore entail the product of one PDF evaluated at a large value of x with another at a small x. Furthermore, PDFs at large x and small factorization scale Q evolve via the QCD evolution equations to lower x and higher Q, so that large-x uncertainties in fixed-target experiments can have significant consequences for collider measurements [6, 7].

In an effort to obtain constraints on PDFs at large values of x, a study was made by Accardi *et al.* [8] in which the Q^2 and W^2 cuts applied to DIS data were systematically relaxed, thereby allowing data at higher x and lower Q^2 to be used. This necessitated the inclusion of various corrections subleading in $1/Q^2$, such as target mass corrections and higher twist contributions, which become increasingly important as Q^2 is lowered and x tends to 1.

A goal of global PDF fits is to determine the x and Q^2 dependence of the different parton species (gluons, individual quark and antiquark flavors). Charged-lepton DIS experiments on proton targets are sensitive at large x to the combination $4u + d$, but to separate the u and d PDFs an additional constraint is needed. Data on a free neutron target at large values of x would constrain $4d + u$; however, the closest one can come to this is to utilize a deuterium target. Since the proton and neutron in deuterium are not free, it is necessary to account for nuclear effects such as Fermi motion, binding, and nucleon off-shell corrections, which can be significant at large values of x. Estimates of the uncertainties due to different models of these nuclear corrections were studied in Ref. [11].

The purpose of the present paper is to synthesize the lessons of the previous studies [8, 11], and present three sets of global next-to-leading order (NLO) PDF fits, each of which differs by the size of the nuclear corrections employed for the deuteron target DIS data. The results are referred to collectively as the CJ12 PDFs (with "CJ" denoting the CTEQ-Jefferson Lab collaboration [12]), and the three PDF sets with mild, medium and strong nuclear corrections are designated as "CJ12min", "CJ12mid" and "CJ12max", respectively. These PDFs provide a convenient way to explore the effects of the nuclear corrections on various observables.

In the following section we describe the methodology involved in the fits, including the choices of data sets, the parametrizations used, and the treatment of nuclear and finite-Q^2 corrections. We also discuss the treatment of the experimental errors and the resulting error PDF sets. In Sec. III we present an overview of the CJ12 PDF results, and compare these with results from other global fits. Finally, in Sec. IV we make some concluding remarks and outline plans for future work. An appendix is provided which contains the initial parameter values for each of the PDF sets.

II. FORMALISM AND PROCEDURES

The CJ12 PDF sets described herein result from global fits to a wide variety of data totaling 3958 data points. The global fitting procedures utilize NLO calculations for each observable. For the DIS observables, higher twist contributions and target mass corrections are included, and for the deuterium DIS data sets nuclear corrections are taken into account, as described in this section.

A. Data

The data sets used, listed in Table I, encompass data ranging from medium energy electron-hadron scattering at Jefferson Lab to high-energy hadron-hadron scattering at the Fermilab Tevatron. The kinematic cuts employed in this analysis, $Q^2 > Q_0^2 = (1.3\ \mathrm{GeV})^2$ and $W^2 > 3\ \mathrm{GeV}^2$, allow the inclusion of: F_2 structure function measurements on hydrogen and deuterium from BCDMS [13], SLAC [16], NMC [14, 15], and Jefferson Lab [17]; neutral current (NC) and charged current (CC) DIS cross sections from HERA [18]; Drell-Yan data from Fermilab [19]; W (and decay lepton) asymmetries from CDF and DØ [20–24]; Z rapidity distributions from CDF and DØ [25, 26]; jet production cross sections from both CDF [27, 28], and DØ [29, 30], and photon plus jet production from DØ [31].

DIS data with a deuterium target are necessary for u and d quark flavor separation at large x, which entails the use of nuclear corrections, as will be discussed and evaluated below. Unlike global fits from other groups, the present data set does not include the NuTeV dimuon data [32] from neutrino-iron scattering, which provide essentially the only currently available source of information on the s and $\bar{s}$ quark distributions (except possibly for W and Z production at the LHC [33]). The reason is that, beside corrections due to modifications of medium-x quark PDFs in the heavy nuclear target, which are generally not too large [34–38], the uncertainty due to in-medium propagation of the tagged final state charm quark and D meson may be significant [39]. Similarly, we do not use E605 data on dimuon production from a copper target [40], and rely on E866 data [19] only to constrain antiquark distributions.

The x and Q^2 coverage of these data is illustrated in Fig. 1, where leading order kinematics was used according to the procedure detailed in Ref. [41]. While nominally there is a substantial amount of data at large x from vector boson production measurements, only the directly reconstructed $W^{\pm}$ charge asymmetry data from the CDF collaboration has a sufficient statistical precision to constrain the d quark distribution uncertainty to the level aimed for in this study. Note that the lepton charge asymmetry data also have high precision; however, the lepton decay smears the primary W production process, resulting in an effective large-x reach smaller than that for the W asymmetry. The remaining source of large-x data is DIS, for which the kinematic cuts used in this work are comparable to those in the global fits of Alekhin *et al.* [42, 43], but lower than the typical cuts used in all

TABLE I: Data sets and number of data points used in the global fits, together with the χ^2 values for each of the CJ12min, CJ12mid and CJ12max fits.

				χ^2		
	Experiment	Ref.	# points	CJ12min	CJ12mid	CJ12max
DIS F_2	BCDMS (p)	[13]	351	434	436	437
	BCDMS (d)	[13]	254	294	297	302
	NMC (p)	[14]	275	434	432	430
	NMC (d/p)	[15]	189	179	177	182
	SLAC (p)	[16]	565	456	455	456
	SLAC (d)	[16]	582	394	388	396
	JLab (p)	[17]	136	170	169	170
	JLab (d)	[17]	136	124	125	126
DIS σ	HERA (NC e^-)	[18]	145	117	117	118
	HERA (NC e^+)	[18]	384	595	596	596
	HERA (CC e^-)	[18]	34	19	19	19
	HERA (CC e^+)	[18]	34	32	32	32
Drell-Yan	E866 (p)	[19]	184	220	221	221
	E866 (d)	[19]	191	297	307	306
W asymmetry	CDF 1998 (ℓ)	[20]	11	14	16	18
	CDF 2005 (ℓ)	[21]	11	11	11	10
	DØ 2008 (ℓ)	[22]	10	4	4	4
	DØ 2008 (e)	[23]	12	40	36	34
	CDF 2009 (W)	[24]	13	20	25	41
Z rapidity	CDF (Z)	[25]	28	29	27	27
	DØ (Z)	[26]	28	16	16	16
jet	CDF run 1	[27]	33	52	52	52
	CDF run 2	[28]	72	14	14	14
	DØ run 1	[29]	90	21	20	19
	DØ run 2	[30]	90	19	19	20
γ+jet	DØ 1	[31]	16	6	6	6
	DØ 2	[31]	16	13	13	12
	DØ 3	[31]	12	17	17	17
	DØ 4	[31]	12	17	16	17
TOTAL			3958	4059	4055	4096
TOTAL + norm				4075	4074	4117

other other global PDF analyses [44–48]. The improvement in the large-x kinematic reach is significant, amounting to about 1300 more data points roughly equally divided between proton and deuteron targets, with adequate precision. This represents some $\sim 50\%$ increase in the total number of DIS data points compared with the standard cuts.

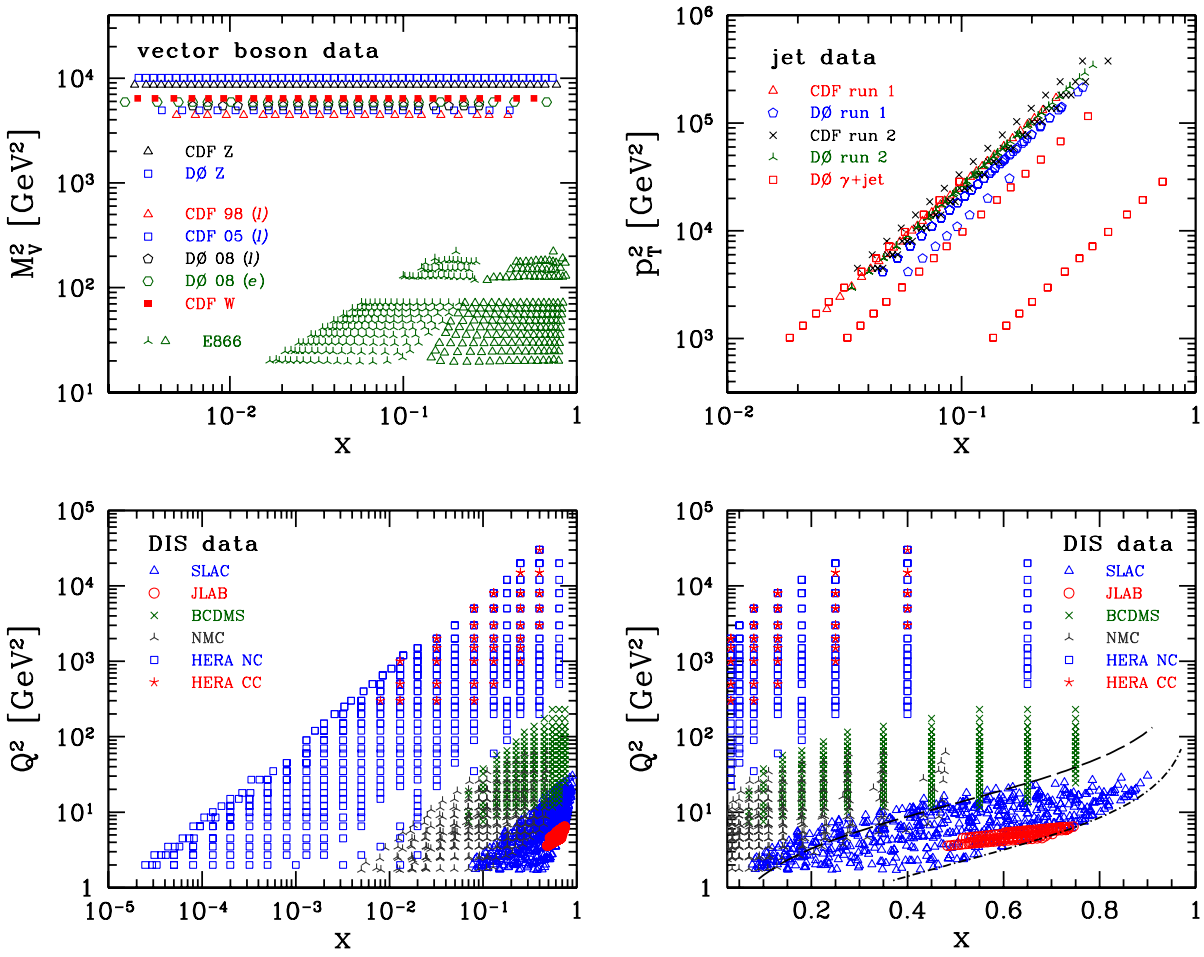

FIG. 1: Nominal coverage of the data sets used in the CJ12 global fits. *Top row*: vector boson and jet production. In the vector boson data plot, M_V is the mass of the boson, and the weak boson data have been offset vertically for clarity. For the E866 dimuon data, the 3-pointed star and open triangle symbols correspond to the target and projectile x values, respectively. In the jet data plot, p_T is the transverse momentum of the jet. *Bottom row*: DIS data on a logarithmic and linear x scale. In the latter, the $W^2 \gtrsim 14$ GeV^2 cut typically used in global PDF fits and the $W^2 > 3$ GeV^2 cut used in this analysis are indicated by the dashed and dot-dashed lines, respectively.

B. PDF parametrizations and conventions

The calculations used in this analysis are all performed at NLO. Correspondingly, the PDFs are evolved from the input scale Q_0^2 using NLO splitting functions. It would be possible to utilize NNLO splitting functions and, indeed, for some of the processes the hard scattering cross section expressions are known to NNLO. However, this is not true for the

jet and γ + jet processes. In order to not mix NLO and NNLO treatments of data sets, we will for consistency treat all fitted process at NLO.

For the Q^2 evolution, we use a zero-mass variable flavor scheme with the charm and bottom flavor thresholds set at $m_c = 1.3$ GeV and $m_b = 4.5$ GeV, respectively. In this scheme, the only explicit dependence on the quark masses is the value at which the number of active flavors changes. While it is true that various schemes exist for taking into account the kinematic effects of nonzero quark masses in DIS [46], those schemes have not been extended to the other processes that have been included in this analysis. Accordingly, we choose the zero-mass scheme so that the PDFs can be treated consistently for each observable.

The fits described herein were all performed using a value of $\Lambda^{(5)} = 0.2268$ GeV for 5 active flavors, corresponding to the value $\alpha_s(M_Z) = 0.1180$ at two-loop accuracy. This choice is based on the world average of $\alpha_s = 0.1184 \pm 0.0007$ [51]. Of course, one can also treat Λ as a free parameter; doing so, we find that the fitted Λ results in a value $\Lambda^{(5)} = 0.2278 \pm 0.0016$ GeV, consistent with our fixed value. However, the present analysis focusses on effects on the PDFs due to the inclusion of the nuclear corrections for deuterium data. Accordingly, we chose a fixed value of $\alpha_s(M_Z)$ specifically to avoid having the coupling determined by one or more of the higher statistics data sets. We intend to return to this issue in a future analysis by scanning a range of $\alpha_s(M_Z)$ values in order to understand the effects on individual data sets.

For the parametrization of the PDFs at the input scale Q_0^2, a common form has been adopted for all parton species f,

$$xf(x, Q_0^2) = a_0 x^{a_1}(1-x)^{a_2}(1 + a_3\sqrt{x} + a_4 x). \tag{1}$$

This form applies to the valence distributions $xq_v \equiv x(q - \bar{q})$, for $q = u$ and d, the isoscalar and isovector sea quark distributions $x(\bar{u} + \bar{d})$ and $x(\bar{d} - \bar{u})$, and the gluon distribution xg. However, to allow for a more flexible parametrization of the valence d_v PDF in the large-x region, we add in a small admixture of the u_v PDF,

$$d_v \to a_0^{d_v}\left(\frac{d_v}{a_0^{d_v}} + b\, x^c u_v\right), \tag{2}$$

with b and c as two additional parameters. The result of this modification is that $d_v/u_v \to a_0^{d_v}\, b$ as $x \to 1$, provided $a_2^{d_v} > a_2^{u_v}$, which is usually the case. A finite, nonzero value of

this ratio is indeed expected in several nonperturbative models of hadron structure [3–5]. It is also required from a purely practical point of view, as it avoids potentially large biases on the d-quark PDF central value [11], as well as on its PDF error estimate, as we discuss in detail in Sec. III. The a_0 parameters for the u_v and d_v distributions are fixed by the appropriate valence quark number sum rules, while a_0^g is fixed by the momentum sum rule. Finally, since we do not use neutrino–nucleus DIS data in the fits, the strange quark PDF is assumed to be proportional to the isoscalar light quark sea, and parametrized as

$$(s + \bar{s}) = \kappa(\bar{u} + \bar{d}). \tag{3}$$

The possibility of asymmetric s and $\bar{s}$ distributions, predicted in several nonperturbative models [49, 50], can be investigated using dimuon data in neutrino and antineutrino DIS [32], and will be the subject of future analysis including nuclear corrections for heavy nuclei. The parameter values for each of the three PDF sets (CJ12min, CJ12mid and CJ12max) are given in Table II in Appendix A.

We find that the parametrization (1) is sufficiently flexible to allow good fits to the combined data sets, with typical χ^2 values on the order of one per degree of freedom, as shown in Table I. In some instances the parameters were found to have very large errors, indicating that the chosen data sets were unable to provide sufficiently strong constraints in those cases. Such parameters were fixed at suitable values, and included in the fits at the values shown in Table II without errors.

C. Target mass and higher twist corrections

The standard method to calculate target mass corrections (TMCs) in DIS is the one based on the operator product expansion in QCD, first formulated by Georgi and Politzer [52]. An alternative method based on collinear factorization in momentum space was developed by Ellis, Furmanski and Petronzio [53], and extended by various authors [54–56] (see also the recent reviews of TMCs in Refs. [57, 58]). All of these methods suffer to some extent from the threshold problem, whereby the target mass corrected structure function remains nonzero as $x \to 1$ [59–61]. For the purposes of global fits, however, the region where the threshold effects become problematic is $W \lesssim 2$ GeV [61], which is mostly outside of where even the most liberal cuts in W and Q^2 are made [8, 11, 42].

According to the classic works of De Rújula *et al.* [62, 63], the appearance of the threshold problem is attributed to the neglect of dynamical higher twist (HT) corrections, which scale as powers in $1/Q^2$. Moreover, higher order perturbative QCD corrections can also resemble power suppressed contributions at low Q^2. Regardless of their origin, we can account for the various power suppressed corrections that are not included in a leading twist calculation by parametrizing them using a phenomenological multiplicative factor, as in the earlier CJ fits [8, 11],

$$F_2(x,Q^2) = F_2^{\rm LT}(x,Q^2)\left(1+\frac{C(x)}{Q^2}\right), \tag{4}$$

where $F_2^{\rm LT}$ denotes the leading twist structure function including TMCs. For simplicity we generically refer to the fitted $1/Q^2$ term as a "higher twist" correction, and parametrize the higher twist coefficient function by $C(x) = a_{\rm HT}\, x^{b_{\rm HT}}(1 + c_{\rm HT}x)$, assuming it to be isospin independent (see, however, Refs. [64–67]).

With the inclusion of TMCs and a phenomenological HT correction, it was found in Ref. [8] that the leading twist PDFs are essentially independent of the TMC prescription adopted; the HT parameters were able to compensate for the variations due to the different TMC algorithms. While the focus in the present work is on the leading twist PDFs, the interpretation and isospin dependence of the higher twist corrections are of intrinsic interest in their own right, and will be the subject of a future dedicated analysis.

D. Nuclear corrections

Since nucleons bound in a nucleus are not free, the nuclear structure function deviates from a simple sum of free proton and neutron structure functions, especially at large x where the effects of Fermi motion, nuclear binding, and nucleon off-shellness are most prominent. In the nuclear impulse approximation the structure function of the deuteron d can be expressed as a convolution of the bound nucleon structure function and a momentum distribution $f_{N/d}$ of nucleons in the deuteron [68–70],

$$F_2^d(x,Q^2) \;=\; \sum_{N=p,n}\int dz\, f_{N/d}(z,\gamma)\, F_2^N(x/z,Q^2) \;+\; \delta^{(\rm off)}F_2^d(x,Q^2), \tag{5}$$

where the additive term $\delta^{(\rm off)}F_2^d(x,Q^2)$ represents nucleon off-shell and relativistic corrections that cannot be expressed through a one-dimensional convolution. The momentum

distribution, or "smearing function", $f_{N/d}$ is computed in the weak binding approximation (WBA), which is appropriate for a weakly bound nucleus such as the deuteron, in terms of the deuteron wave function, and implements nuclear binding and Fermi motion effects [70, 71]. At $Q^2 \to \infty$ it has a simple probabilistic interpretation in terms of the light-cone momentum fraction $z = (M_d/M)(p \cdot q/p_d \cdot q) \approx (M_d/M)(p^+/p_d^+)$ of the deuteron carried by the struck nucleon, where p and p_d are the four-momenta of the nucleon and deuteron, respectively, and M_d is the deuteron mass. At finite Q^2, however, the smearing function depends in addition on the parameter $\gamma^2 = 1 + 4x^2M^2/Q^2$, which characterizes the deviation from the Bjorken limit.

The nuclear corrections at large x depend partly on the strength of the high-momentum tail of the deuteron wave function, and we use several wave functions based on different nucleon–nucleon potentials to study the deuteron model dependence. We choose the high-precision AV18 [72], CD-Bonn [73] and the relativistic WJC-1 [74] wave functions, which provide a representative spread of behaviors at high momentum. Note that the effects of the nuclear smearing corrections are not suppressed at large Q^2, and must be considered at all scales wherever data at $x \gtrsim 0.5$ are used [8–10].

The off-shell nucleon correction $\delta^{(\text{off})}F_2^d$ is somewhat more model dependent, but several quark model based estimates of this have been made in the literature [70, 75–77]. In this work we follow the approach adopted in our previous analysis [11], which utilized the "modified Kulagin-Petti" model. In this model, the corrections were related to the change in the nucleon's confinement radius in the nuclear medium, as well as the average virtuality of the bound nucleons, and constrained to give no net change in the structure function normalization. In contrast to Ref. [11], however, here we further take into account the correlation between the nucleon "swelling" and the deuteron wave function. The combined effects introduce a theoretical uncertainty in the extracted PDFs, particularly for the d quark. A detailed evaluation of the impact of this uncertainty will be presented in Sec. III.

E. PDF Errors

The global fits were performed using a standard χ^2 minimization algorithm due to Marquardt [78], as described in Ref. [79]. This prescription produces a well-defined Hessian matrix typically in fewer than a dozen iterations and is both efficient and well-behaved.

Where available, correlated systematic errors have been utilized. Error PDF sets were produced using the resulting Hessian following the methods described in Ref. [80]. Two error PDFs were produced for each of the eigenvalues of the Hessian, corresponding to positive and negative parameter increments, resulting in a total of 38 error PDFs for each of the three choices of nuclear corrections.

Using these error PDFs it is possible to construct an error estimate $\delta\sigma$ for some physical observable σ via

$$\delta\sigma = \frac{T}{2}\sqrt{\sum_{i=1}^{19}\Big[\sigma(a_{2i-1}) - \sigma(a_{2i})\Big]^2}, \tag{6}$$

where a_i denotes the set of parameters corresponding to the PDF set i, and T is a χ^2 tolerance that will be described below. Alternatively, one can define asymmetric upper and lower errors $\delta\sigma_+$ and $\delta\sigma_-$ based on the same error PDF sets using the expressions

$$\delta\sigma_+ = T\sqrt{\sum_{i=1}^{19}\Big(\max\Big[\sigma(a_{2i-1}) - \sigma(a), \sigma(a_{2i}) - \sigma(a), 0\Big]\Big)^2}, \tag{7a}$$

$$\delta\sigma_- = T\sqrt{\sum_{i=1}^{19}\Big(\max\Big[\sigma(a) - \sigma(a_{2i-1}), \sigma(a) - \sigma(a_{2i}), 0\Big]\Big)^2}, \tag{7b}$$

where $\sigma(a)$ denotes the observable calculated with the "central value" of the fitted PDF set.

The issue of the appropriate value for the χ^2 tolerance T has been discussed at length in the literature. The value $T = 1$ is suitable in the case where all data sets are compatible with each other and all errors are Gaussian. In practice, various tolerance values are used in different PDF analyses, including $T = 10$ for the CTEQ6 PDFs [80], $T = \sqrt{50}$ in the MRST2002 fits [81], and dynamically determined values in more recent fits [44, 45]. In the CJ12 analysis discussed in this paper the error bands have been calculated using $T = 10$.

F. Theoretical errors

A significant source of theoretical errors is the modeling of nuclear corrections for DIS on deuterium targets, which we refer to as "nuclear uncertainty" in short. Of course, since the deuteron can never be considered as composed of free nucleons, it is never physically reasonable to assume no nuclear corrections at all. We evaluate the nuclear uncertainty by considering nuclear corrections ranging from mild, corresponding to the hardest of the

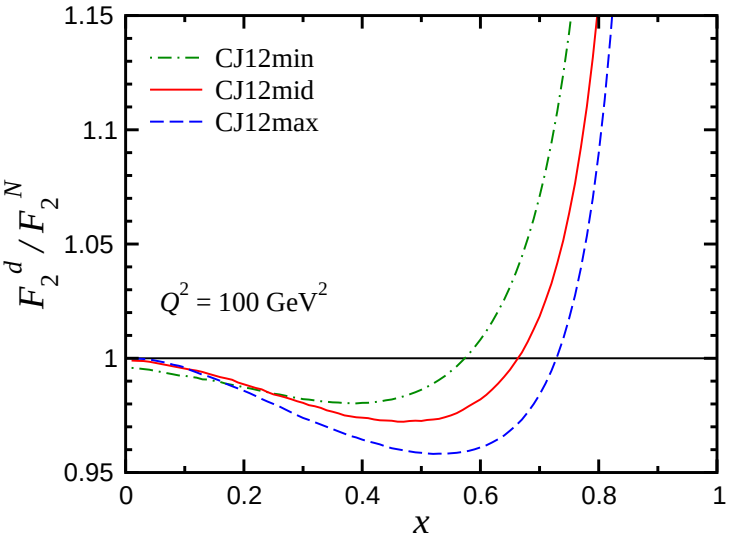

FIG. 2: Ratio of deuteron to isoscalar nucleon structure functions F_2^d/F_2^N for the three sets of nuclear corrections considered in this analysis, corresponding to the CJ12min (dot-dashed), CJ12mid (solid), and CJ12max (dashed) PDFs.

modern deuteron wave functions (WJC-1 [74]) coupled to a 0.3% nucleon swelling effect, to strong, corresponding to the softest of the wave functions (CD-Bonn [73]) and a large, 2.1% nucleon swelling. An intermediate nuclear correction corresponding to the AV18 [72] deuteron wave function and a 1.2% nucleon swelling effect is taken for our central fit. These corrections approximately span the same range as in our previous analysis [11].

The effect of the different nuclear corrections is illustrated in Fig. 2 for the ratio of F_2 structure functions of the deuteron and an idealized isoscalar target consisting of an unbound proton and neutron. The upper, middle, and lower curves are the results for the mild (CJ12min), intermediate (CJ12mid), and strong (CJ12max) nuclear corrections. An intuitive way to understand the effects of these nuclear corrections on global fits is to consider the idealized free proton plus neutron target as being obtained by dividing the deuterium target data by the ratio shown in Fig. 2. In the intermediate-x region the idealized nucleon F_2^N structure function is larger than the original data, and the increase is largest for the maximum nuclear correction model. On the other hand, as one extends to values of x above about 0.75, the reverse is true: the F_2^N results there lie below the data and are lowest for the mild set of corrections.

In a global fit, it is the combination of PDFs and nuclear corrections which is constrained

by deuterium data, not the PDFs alone. At large x, the u quark is well constrained by free proton DIS and other data, so that when fitting the corrected deuterium data (essentially the idealized $F_2^N \propto u + d$) the d quark will be the distribution most sensitive to the nuclear corrections. Therefore, in the large-x region the d PDF will be smallest for the mild correction and largest for the strong corrections (see Fig. 7 in Sec. III).

One way to evaluate the impact of the nuclear uncertainty on a given observable is by calculating it using the CJ12min fit corresponding to the smallest nuclear correction, then with the CJ12max fit corresponding to the largest correction. The values of the observable spanning these 2 extremes can be considered a fair representation of the theoretical nuclear uncertainty. PDF errors can then be added to the central values so calculated, and displayed as an outer error band, as done in Ref. [8, 11]. Alternatively, one could first calculate a PDF error band using the CJ12mid set, and display this on top of the 2 bands obtained with the min and max sets. The size of the resulting sidebands will then represent the nuclear uncertainty.

III. RESULTS

In this section the results of the CJ12min, CJ12mid, and CJ12max sets of global PDF fits are presented and compared with other modern PDF fits. Tables for the central PDF sets, the corresponding error PDF sets, and a user interface to read them can be found on the CJ [12] and CTEQ [82] web sites.

The data sets used in the global fits are shown in Table I along with the χ^2 values of the three fits for each of the data sets used in the analysis, as well as the total χ^2 values and the totals with the normalization contribution to the χ^2 included. As is apparent from these values, the description of most of the data sets is independent of the size of the nuclear corrections. Indeed, the deuterium data are sensitive to the convolution of the nuclear model with the d PDF; as the model is changed, the d PDF is altered by the fitting program to compensate. For observables such as the jet cross section, the modified d PDF can be compensated for by small changes in the gluon PDF, so the overall description of the data remains unaltered. One notable exception to this pattern is for the W asymmetry as measured by the CDF collaboration [24]. This observable is sensitive to the d/u ratio, and changes in the d PDF are not easily compensated by the u PDF, which is relatively

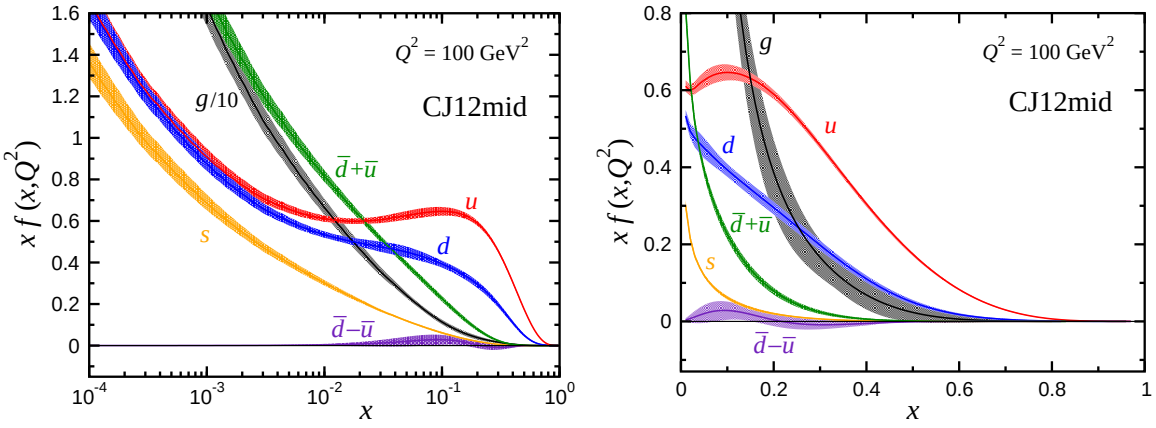

FIG. 3: Uncertainty bands for the u, d, $\bar{d}+\bar{u}$, $\bar{d}-\bar{u}$, s and g PDFs for the CJ12mid fit at $Q^2 = 100$ GeV^2, shown on logarithmic (left) and linear (right) scales in x. Note that in the left panel the gluon is scaled by 1/10.

well constrained by proton DIS data. The χ^2 for the W asymmetry data does show a significant increase as the magnitude of the nuclear corrections increases beyond its middle value, indicating a preference for mild to medium nuclear corrections.

In this regard it is interesting to compare our results to those of the recent analysis in Ref. [83], which included nuclear corrections for deuterium targets in DIS using a 4-parameter, Q^2-independent phenomenological function with the parameters varied in the fit. The resulting correction factor, shown in Fig. 11 of Ref. [83], can be compared to those in Fig. 2 above. Their fitted form lies between the curves for the CJ12min and CJ12mid fits, as might be expected since these two fits have nearly identical values for χ^2, while the CJ12max value is higher. As noted above, much of the increase in χ^2 for the CJ12max set is due to the CDF W asymmetry data, which is also included in the fit of Ref. [83]. Although this comparison is not exact, since our nuclear corrections are Q^2 dependent [84] and those in Ref. [83] are not, it is consistent with our observation that the nuclear model choices made for the CJ12min and CJ12mid sets are preferred by the data.

The CJ12mid PDFs are shown in Fig. 3 at $Q^2 = 100$ GeV^2 with the PDF error bands calculated as described in Sec. II E, on both logarithmic and linear x scales. The latter more graphically illustrates the behavior of the PDFs at large values of x, where the uncertainties from nuclear and finite-Q^2 corrections are greatest. The error bands are shown in more detail in Fig. 4, and compared to the CJ12min and CJ12max sets. It is clear that the effects of nuclear corrections are strongest on the d PDF, with the others showing little or

no influence. In particular, the d quark PDF increases at large values of x as the magnitude of the nuclear corrections increases. This, again, is a reflection of the fact that it is the convolution of the nuclear corrections and the d PDF that is constrained by the deuterium DIS data, and not the d PDF alone.

A comparison of the CJ12mid PDFs with several other sets is shown in Fig. 5, which for illustration includes the CT10 [45], MSTW08 [44] and ABKM09 [42] PDFs. The latter in particular are closest in spirit to the CJ12 PDFs in that similar kinematic cuts are imposed, and nuclear and finite-Q^2 corrections included, albeit using somewhat different prescriptions. One feature that is readily apparent in the first two panels is that the error bands for the u and d PDFs are reduced relative to those from the other sets. This is a direct consequence of the lower cuts on Q^2 and W^2 which allow DIS data to be fitted to larger values of x, approaching 0.9. Of course, when one considers the variations allowed by the different nuclear models, the error bands again increase, modestly for the u quark and substantially for the d quark.

To further examine the role of the deuteron DIS data, a global fit was performed with the deuterium DIS points removed from the data set. The results are shown in Fig. 6 for the u and d PDFs relative to those from the CJ12mid set. Without the deuterium data the error band for the u PDF shows a modest increase beyond $x \approx 0.7$, while that for the d PDF shows a significant increase over most of the x range. It is important to note that the error band on the d PDF without the deuterium data exceeds the band which includes the nuclear uncertainties. This clearly demonstrates the usefulness of the deuterium DIS data, even in the presence of the nuclear uncertainties that its use introduces.

For the strange quark PDF, the error band shown is somewhat smaller than for other sets. This is an artificial reduction, however, since we do not use the NuTeV dimuon DIS data [32], which are taken on heavy nuclear targets. Accordingly, the value of κ in Eq. (3) is fixed, rather than fitted, and the error on the $s + \bar{s}$ combination is therefore proportional to that of $\bar{u} + \bar{d}$. In practice, we use the value $\kappa = 0.4$ from earlier CTEQ fits [80, 85] that employed the same choice for Q_0 as in this analysis. Methods of constraining the s PDF without the use of heavy nuclear targets will be the subject of future investigation.

The ratios of the d to u PDFs for the three CJ12 sets are shown in Fig. 7, which also compares the CJ12mid results with those from the other PDF sets in Fig. 5. Conventional parametrizations that treat the d and u PDFs with the same $(1-x)^{a_2}$ form for the $x \to 1$

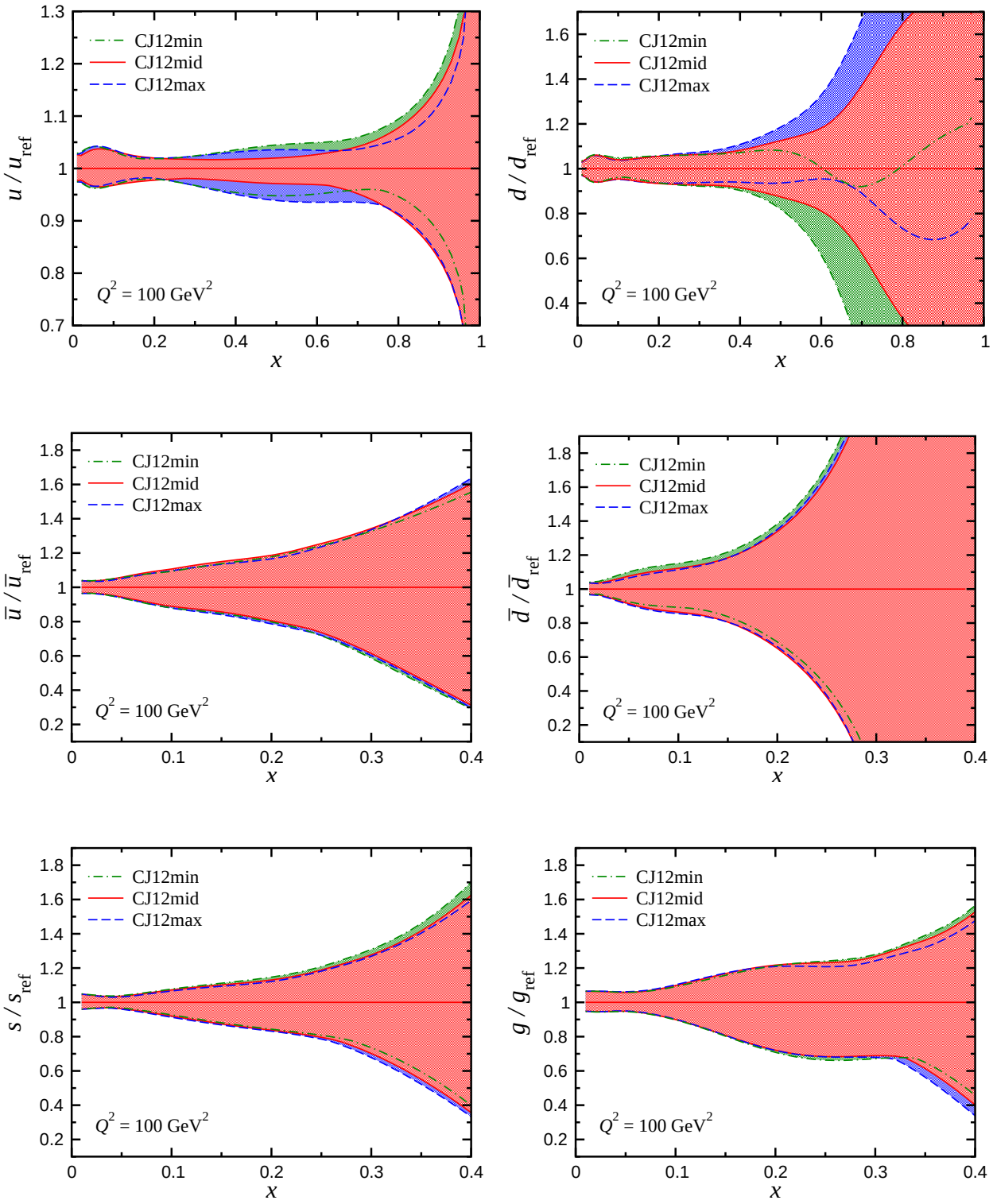

FIG. 4: PDF uncertainties for the CJ12min (dot-dashed), CJ12mid (solid), and CJ12max (dashed) PDF sets relative to the reference CJ12mid set at $Q^2 = 100$ GeV^2.

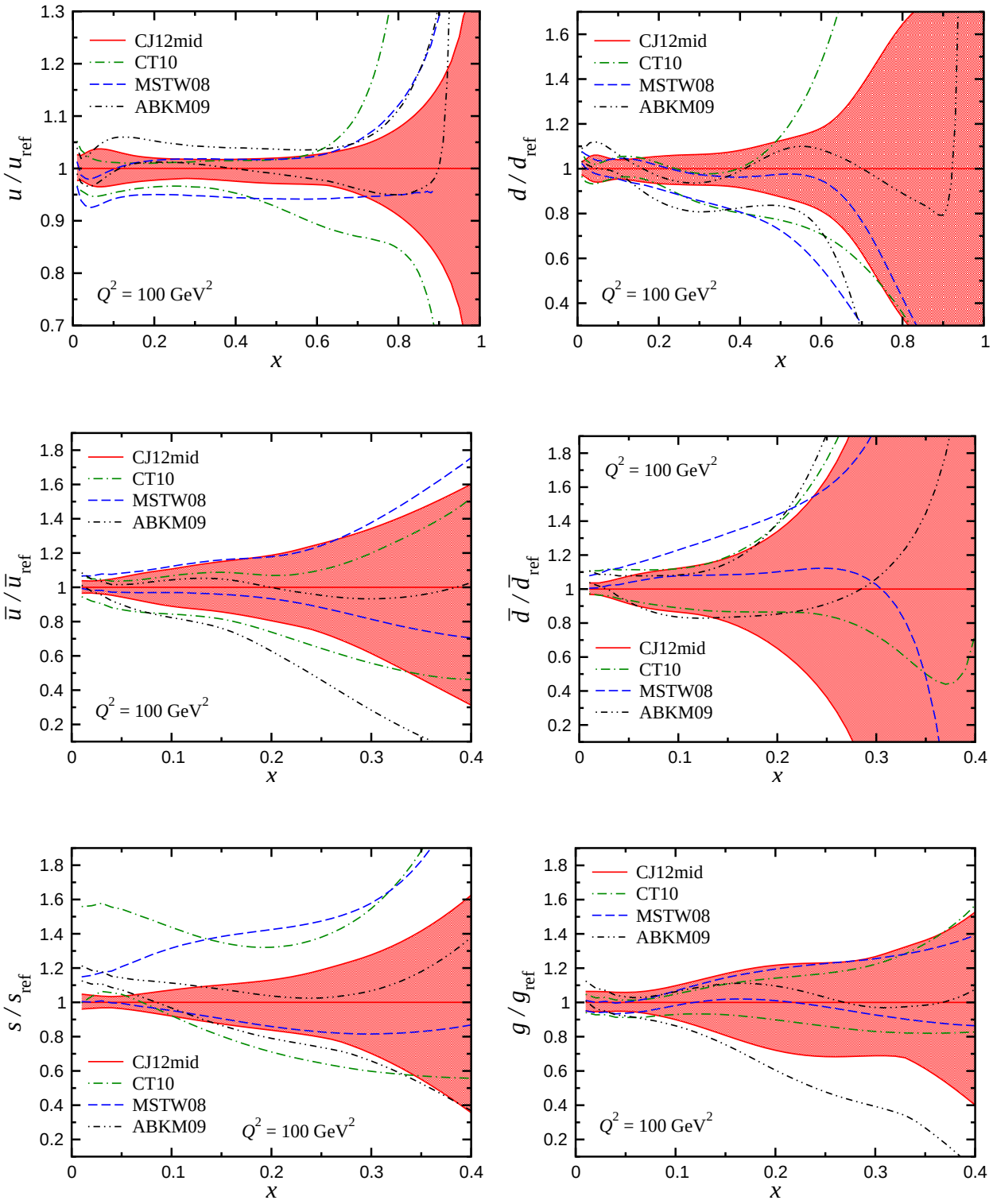

FIG. 5: PDF uncertainties for the CJ12mid (solid), CT10 (dot-dashed), MSTW08 (dashed) and ABKM09 (dot-dot-dashed) PDF sets relative to the reference CJ12mid set at $Q^2 = 100$ GeV^2.

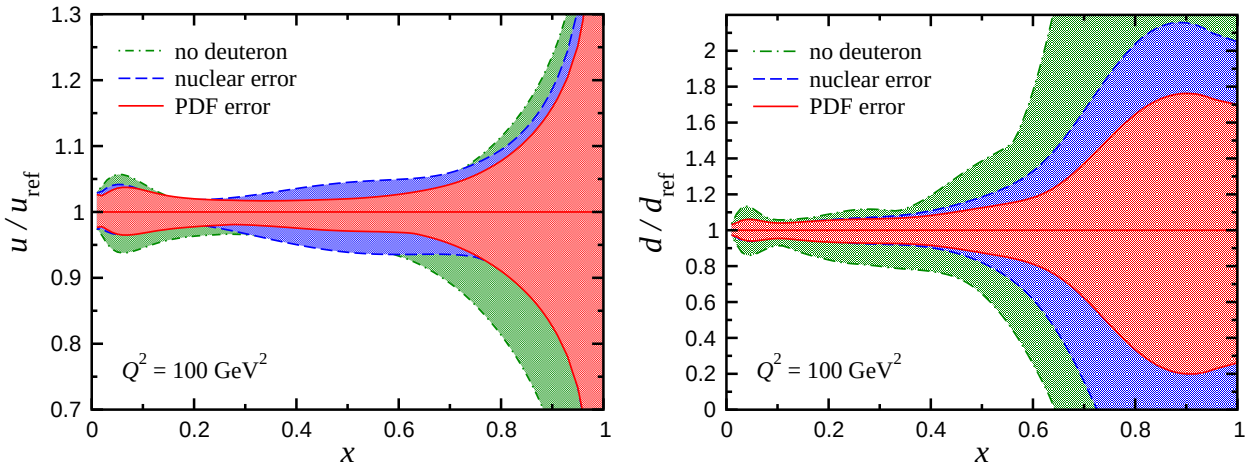

FIG. 6: PDF uncertainties for the CJ12mid u and d quark PDFs (solid) compared with the total uncertainty from nuclear corrections (dashed) and with a fit excluding all deuterium data (dot-dashed), relative to the reference CJ12mid set at $Q^2 = 100$ GeV^2.

behavior, have the characteristic that the d/u ratio tends either to zero or infinity as x approaches one. Conversely, the use of the parametrization given in Eq. (2) allows d/u to have any finite limiting value as $x \to 1$. This is clear from the results in Fig. 7(b), where the MSTW08 and ABKM09 d/u ratios tend to zero, while that for CT10 tends to infinity. This behavior distorts the error bands so that the MSTW08 ratio appears to have an anomalously small uncertainty, while the CT10 result is much larger. However, as the relative errors in Fig. 7(c) show, the MSTW08 and CT10 bands are similar, as would be expected, while the CJ12 and ABKM09 bands are somewhat reduced in size at larger values of x due to the additional high-x data used in those analyses. The ABKM09 band then diverges again from the CJ12 band because of the use of a conventional d quark parametrization.

As the magnitude of the nuclear corrections increases, the value of the d/u intercept at $x = 1$ rises because of the mechanism discussed in Sec. II D. The central values of d/u extrapolated to $x = 1$ are 0.012, 0.22, and 0.33 for the CJ12min, CJ12mid, and CJ12max fits, respectively. Including the PDF errors we find

$$d/u \underset{x\to 1}{\longrightarrow} 0.22 \pm 0.20\,(\text{PDF}) \pm 0.10\,(\text{nucl}), \tag{8}$$

where the first error is from the PDF fits and the second is from the nuclear correction models. These values encompass the range of available theoretical predictions [1–5]. However, it is also clear that a relatively modest improvement in statistical precision and reduction of

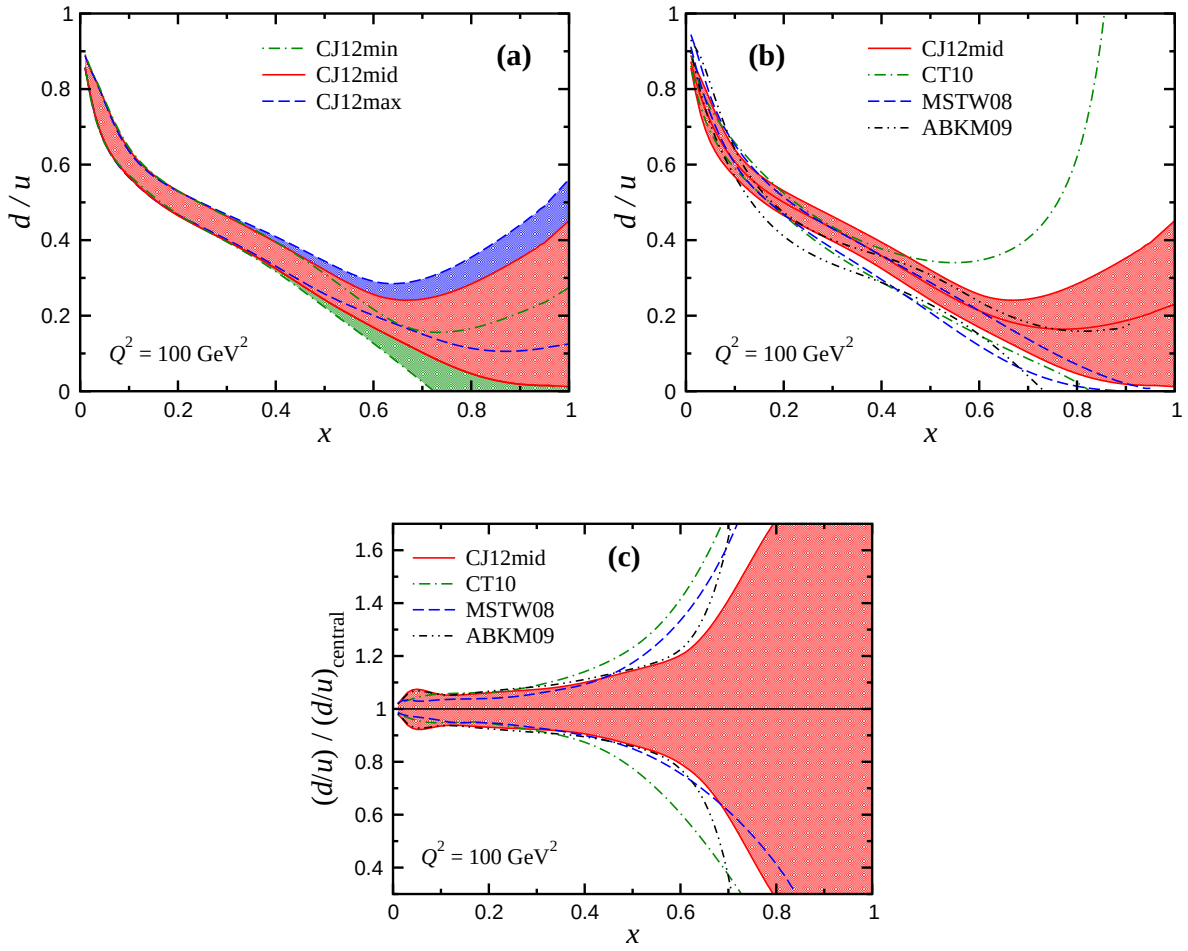

FIG. 7: d/u ratio at $Q^2 = 100$ GeV^2 for (a) the CJ12min (dot-dashed), CJ12mid (solid) and CJ12max (dashed) PDFs, (b) the CJ12mid (solid), CT10 (dot-dashed), MSTW08 (dashed) and ABKM09 (dot-dot-dashed) PDFs, and (c) relative to the central values of d/u for each PDF set.

nuclear uncertainty would allow one to restrict the range of allowable physical mechanisms.

IV. CONCLUSION

The CJ12 next-to-leading order PDFs presented in this study demonstrate the clear necessity of including nuclear corrections in global fits for PDFs when deuterium DIS data are included. The largest effect is on the d quark PDF, where variations can be observed for values of $x \gtrsim 0.5$. The theoretical uncertainty accompanying these corrections is of the same order of magnitude as the PDF uncertainty, and the CJ12 PDF sets will enable one to assess the impact of nuclear effects on the error bands estimated for various observables. The

impact of these corrections is important for observables that depend on PDFs at moderate to large values of x, such as the production of high mass states and cross sections at large values of rapidity. Examples of such effects for selected observables at the Tevatron and LHC were recently discussed in Ref. [7].

The CJ12 fits utilize an expanded DIS data set obtained by relaxing the kinematic cuts to $Q^2 > Q_0^2 = (1.3 \text{ GeV})^2$ and $W^2 > 3 \text{ GeV}^2$, and considering finite-Q^2 corrections such as target mass and higher twist effects in the theoretical calculations. The resulting significant improvement in the statistics of the DIS data at large x more than compensates for the nuclear correction uncertainty, resulting in a net improvement in the precision to which the d quark is extracted from experimental data.

The PDFs presented in this analysis form a baseline for comparisons to be done in further studies, and there are a number of issues to be investigated. For example, we would like to determine the effects on individual data sets of changing the $\alpha_s(M_Z)$ value used in the fit. Similarly, we envision a dedicated study of the effects of choosing different conventions for treating heavy quarks in DIS processes and of including nuclear corrections for other observables.

Further refinements of the CJ12 PDFs are anticipated as additional data become available. One natural extension is to assess the constraints provided by the addition of new LHC data to the global fits, such as on the s quark distribution [33]. Additional constraints on other PDFs may be provided through Z rapidity measurements [86], and high-p_T jet and direct photon production [87]. A dedicated study of the impact of longitudinal structure function measurements at Jefferson Lab [88, 89] on large-x gluons is also foreseen. The potential of large rapidity measurements in proton-proton collisions at the upgraded RHIC detectors, or the proposed AFTER@LHC experiment [90] can also be explored.

As new and more precise measurements of observables sensitive to the d-quark in the proton and less sensitive to nuclear corrections become available in the future [91–93], complementing the existing W charge asymmetry data [24], global QCD fits will become capable of constraining theoretical models of nuclear corrections in the deuteron. Not only will this reduce the nuclear uncertainty on the fitted PDFs, it will also provide a new avenue for progress in the theoretical understanding of high-energy processes involving nuclei.

Acknowledgments

We thank M. E. Christy, P. Jimenez-Delgado, C. E. Keppel and P. Monaghan for helpful discussions, and M. E. Christy and S. Malace for assistance with the parametrizations of the nucleon off-shell corrections used here. This work was supported by the DOE contract No. DE-AC05-06OR23177, under which Jefferson Science Associates, LLC operates Jefferson Lab. The work of J.F.O. and A.A. was supported in part by DOE contracts No. DE-FG02-97ER41922 and No. DE-SC0008791, respectively.

Appendix A: Parameter values

In this appendix we list the initial parameter values and their errors for the three sets of PDFs discussed in the text.

TABLE II: Parameter values for the three CJ12 PDF sets at the initial scale $Q_0 = 1.3$ GeV. The parameters without errors have been fixed by sum rules or other constraints.

Parameter	CJ12min	CJ12mid	CJ12max
$a_0^{u_v}$	2.8468	2.7684	2.9343
$a_1^{u_v}$	0.65468 ± 0.02138	0.64839 ± 0.02115	0.66220 ± 0.02152
$a_2^{u_v}$	3.5453 ± 0.0178	3.5686 ± 0.0164	3.5733 ± 0.0175
$a_3^{u_v}$	0.0	0.0	0.0
$a_4^{u_v}$	2.7201 ± 0.4322	2.8970 ± 0.4005	2.6616 ± 0.4266
$a_0^{d_v}$	15.389	21.515	24.724
$a_1^{d_v}$	1.0296 ± 0.0449	1.1004 ± 0.0422	1.1328 ± 0.0420
$a_2^{d_v}$	6.3767 ± 0.1860	6.9525 ± 0.1905	7.1420 ± 0.1947
$a_3^{d_v}$	-3.7930 ± 0.1098	-3.9659 ± 0.0984	-3.9989 ± 0.0949
$a_4^{d_v}$	5.8404 ± 0.2808	5.9770 ± 0.2454	5.9310 ± 0.2326
b	$(0.0787 \pm 0.1648) \times 10^{-2}$	$(1.0379 \pm 0.1688) \times 10^{-2}$	$(1.3464 \pm 0.2187) \times 10^{-2}$
c	2.0	2.0	2.0
$a_0^{\bar{u}+\bar{d}}$	0.12145 ± 0.00491	0.12154 ± 0.00486	0.12366 ± 0.00490
$a_1^{\bar{u}+\bar{d}}$	-0.23390 ± 0.00445	-0.23389 ± 0.00441	-0.23222 ± 0.00438
$a_2^{\bar{u}+\bar{d}}$	9.6939 ± 0.1901	9.7127 ± 0.1917	9.5842 ± 0.1975
$a_3^{\bar{u}+\bar{d}}$	0.0	0.0	0.0
$a_4^{\bar{u}+\bar{d}}$	23.689 ± 1.740	23.228 ± 1.704	21.882 ± 1.649
$a_0^{\bar{d}-\bar{u}}$	90.16 ± 21.18	112.02 ± 25.64	115.65 ± 26.69
$a_1^{\bar{d}-\bar{u}}$	2.5411 ± 0.1428	2.7048 ± 0.1477	2.7408 ± 0.1492
$a_2^{\bar{d}-\bar{u}}$	$a_2^{\bar{u}+\bar{d}} + 2.5$	$a_2^{\bar{u}+\bar{d}} + 2.5$	$a_2^{\bar{u}+\bar{d}} + 2.5$
$a_3^{\bar{d}-\bar{u}}$	0.0	0.0	0.0
$a_4^{\bar{d}-\bar{u}}$	-4.1657 ± 0.1932	-4.2848 ± 0.1953	-4.1870 ± 0.1914
a_0^g	46.911	49.404	51.157
a_1^g	0.61077 ± 0.03228	0.62122 ± 0.03360	0.63027 ± 0.03479
a_2^g	6.1691 ± 0.6198	6.5242 ± 0.6703	6.8007 ± 0.7273
a_3^g	-3.5055 ± 0.1251	-3.5348 ± 0.1337	-3.5298 ± 0.1423
a_4^g	3.5292 ± 0.2777	3.6436 ± 0.3059	3.6777 ± 0.3324
κ	0.4	0.4	0.4
$a_{\rm HT}$	-0.5627 ± 1.3948	-0.5679 ± 1.1627	-0.4992 ± 1.2213
$b_{\rm HT}$	3.3528 ± 0.9203	3.1936 ± 0.8423	3.1712 ± 0.8654
$c_{\rm HT}$	-9.042 ± 20.930	-8.493 ± 16.200	-9.459 ± 21.695

[1] R. P. Feynman, *Photon Hadron Interactions* (Benjamin, Reading, Massachusetts, 1972).

[2] F. E. Close, Phys. Lett. B **43**, 422 (1973).

[3] G. R. Farrar and D. R. Jackson, Phys. Rev. Lett. **35**, 1416 (1975).

[4] W. Melnitchouk and A. W. Thomas, Phys. Lett. B **377**, 11 (1996).

[5] R. J. Holt and C. D. Roberts, Rev. Mod. Phys. **82**, 2991 (2010).

[6] S. Kuhlmann *et al.*, Phys. Lett. B **476**, 291 (2000).

[7] L. T. Brady, A. Accardi, W. Melnitchouk and J. F. Owens, JHEP **1206**, 019 (2012).

[8] A. Accardi, M. E. Christy, C. E. Keppel, P. Monaghan, W. Melnitchouk, J. G. Morfin and J. F. Owens, Phys. Rev. D **81**, 034016 (2010).

[9] J. Arrington, F. Coester, R. J. Holt and T. -S. H. Lee, J. Phys. G **36**, 025005 (2009).

[10] J. Arrington, J. G. Rubin and W. Melnitchouk, Phys. Rev. Lett. **108**, 252001 (2012).

[11] A. Accardi, W. Melnitchouk, J. F. Owens, M. E. Christy, C. E. Keppel, L. Zhu and J. G. Morfin, Phys. Rev. D **84**, 014008 (2011).

[12] The CTEQ-Jefferson Lab (CJ) collaboration website, `http://www.jlab.org/cj`.

[13] A. C. Benvenuti *et al.*, Phys. Lett. B **223**, 485 (1989); *ibid.* B **236**, 592 (1989).

[14] M. Arneodo *et al.*, Nucl. Phys. B **483**, 3 (1997).

[15] M. Arneodo *et al.*, Nucl. Phys. B **487**, 3 (1997).

[16] L. W. Whitlow *et al.*, Phys. Lett. B **282**, 475 (1992).

[17] S. P. Malace *et al.*, Phys. Rev. C **80**, 035207 (2009).

[18] F. D. Aaron *et al.*, JHEP **1001**, 109 (2010).

[19] E. A. Hawker *et al.*, Phys. Rev. Lett. **80**, 3715 (1998); J. Webb, Ph.D. Thesis, New Mexico State University (2002), arXiv:hep-ex/0301031; P. Reimer, private communication.

[20] F. Abe *et al.*, Phys. Rev. Lett. **81**, 5754 (1998).

[21] D. Acosta *et al.*, Phys. Rev. D **71**, 051104(R) (2005).

[22] V. M. Abazov *et al.*, Phys. Rev. D **77**, 011106(R) (2008).

[23] V. M. Abazov *et al.*, Phys. Rev. Lett. **101**, 211801 (2008).

[24] T. Aaltonen *et al.*, Phys. Rev. Lett. **102**, 181801 (2009).

[25] T. Aaltonen *et al.*, Phys. Lett. B **692**, 232 (2010).

[26] V. M. Abazov *et al.*, Phys. Rev. D **76**, 012003 (2007).

[27] T. Affolder *et al.*, Phys. Rev. D **64**, 032001 (2001).

[28] T. Aaltonen *et al.*, Phys. Rev. D **78**, 052006 (2008).

[29] B. Abbott *et al.*, Phys. Rev. Lett. **86**, 1707 (2001).

[30] V. M. Abazov *et al.*, Phys. Rev. Lett. **101**, 062001 (2008).
B. Abbott *et al.*, Phys. Rev. Lett. **86**, 1707 (2001).

[31] V. M. Abazov *et al.*, Phys. Lett. B **666**, 435 (2008).

[32] D. Mason *et al.*, Phys. Rev. Lett. **99**, 192001 (2007).

[33] G. Aad *et al.*, Phys. Rev. Lett. **109**, 012001 (2012).

[34] I. Schienbein, J. Y. Yu, K. Kovarik, C. Keppel, J. G. Morfin, F. Olness and J. F. Owens, Phys. Rev. D **80**, 094004 (2009).

[35] K. Kovarik, I. Schienbein, F. I. Olness, J. Y. Yu, C. Keppel, J. G. Morfin, J. F. Owens and T. Stavreva, Phys. Rev. Lett. **106**, 122301 (2011).

[36] K. J. Eskola, H. Paukkunen and C. A. Salgado, JHEP **0904**, 065 (2009),

[37] D. de Florian, R. Sassot, P. Zurita and M. Stratmann, Phys. Rev. D **85**, 074028 (2012).

[38] M. Hirai, S. Kumano and T. -H. Nagai, Phys. Rev. C **76**, 065207 (2007).

[39] A. Accardi, F. Arleo, W. K. Brooks, D. D'Enterria and V. Muccifora, Riv. Nuovo Cim. **32**, 439 (2010).

[40] G. Moreno *et al.*, Phys. Rev. D **43**, 2815 (1991).

[41] R. D. Ball, L. Del Debbio, S. Forte, A. Guffanti, J. I. Latorre, J. Rojo and M. Ubiali, Nucl. Phys. B **838**, 136 (2010).

[42] S. Alekhin, J. Blümlein, S. Klein and S.-O. Moch, Phys. Rev. D **81**, 014032 (2010).

[43] S. Alekhin, J. Blümlein and S.-O. Moch, Phys. Rev. D **86**, 054009 (2012).

[44] A. D. Martin, W. J. Stirling, R. S. Thorne and G. Watt, Eur. Phys. J. C **63**, 189 (2009).

[45] H.-L. Lai, M. Guzzi, J. Huston, Z. Li, P. M. Nadolsky, J. Pumplin and C.-P. Yuan, Phys. Rev. D **82**, 074024 (2010).

[46] P. Jimenez-Delgado and E. Reya, Phys. Rev. D **80**, 114011 (2009); *ibid.* D **79**, 074023 (2009).

[47] F. D. Aaron *et al.*, JHEP **1001**, 109 (2010).

[48] R. D. Ball *et al.*, Nucl. Phys. B **867**, 244 (2013).

[49] A. I. Signal and A. W. Thomas, Phys. Lett. B **191**, 205 (1987).

[50] W. Melnitchouk and M. Malheiro, Phys. Rev. C **55**, 431 (1997).

[51] J. Beringer *et al.* [Particle Data Group Collaboration], Phys. Rev. D **86**, 010001 (2012),

http://pdg.lbl.gov.

[52] H. Georgi and H. D. Politzer, Phys. Rev. D **14**, 1829 (1976).

[53] R. K. Ellis, R. Petronzio and G. Parisi, Phys. Lett. B **64**, 97 (1976).

[54] S. Kretzer and M. H. Reno, Phys. Rev. D **69**, 034002 (2004).

[55] A. Accardi and J.-W. Qiu, JHEP **0807**, 090 (2008).

[56] A. Accardi, T. Hobbs and W. Melnitchouk, JHEP **0911**, 084 (2009).

[57] I. Schienbein *et al.*, J. Phys. G **35**, 053101 (2008).

[58] L. T. Brady, A. Accardi, T. J. Hobbs and W. Melnitchouk, Phys. Rev. D **84**, 074008 (2011) [Erratum-ibid. D **85**, 039902 (2012)].

[59] K. Bitar, P. W. Johnson and W. K. Tung, Phys. Lett. B **83**, 114 (1979); P. W. Johnson and W. K. Tung, Print-79-1018 (Illinois Tech), *Contribution to Neutrino '79, Bergen, Norway* (1979).

[60] F. M. Steffens and W. Melnitchouk, Phys. Rev. C **73**, 055202 (2006).

[61] F. M. Steffens, M. D. Brown, W. Melnitchouk and S. Sanches, arXiv:1210.4398 [hep-ph].

[62] A. De Rújula, H. Georgi and H. D. Politzer, Phys. Rev. D **15**, 2495 (1977).

[63] A. De Rújula, H. Georgi and H. D. Politzer, Ann. Phys. **103**, 315 (1977).

[64] M. Virchaux and A. Milsztajn, Phys. Lett. B **274**, 221 (1992).

[65] S. I. Alekhin, S. A. Kulagin and S. Liuti, Phys. Rev. D **69**, 114009 (2004).

[66] J. Blümlein and H. Böttcher, Phys. Lett. B **662**, 336 (2008).

[67] J. Blümlein, arXiv:1208.6087 [hep-ph].

[68] W. Melnitchouk, A. W. Schreiber and A. W. Thomas, Phys. Rev. D **49**, 1183 (1994).

[69] S. A. Kulagin, G. Piller and W. Weise, Phys. Rev. C **50**, 1154 (1994).

[70] S. A. Kulagin and R. Petti, Nucl. Phys. A **765**, 126 (2006).

[71] Y. Kahn, W. Melnitchouk and S. A. Kulagin, Phys. Rev. C **79**, 035205 (2009).

[72] R. B. Wiringa, V. G. J. Stoks and R. Schiavilla, Phys. Rev. C **51**, 38 (1995).

[73] R. Machleidt, Phys. Rev. C **63**, 024001 (2001).

[74] F. Gross and A. Stadler, Phys. Rev. C **78**, 014005 (2008); *ibid.* C **82**, 034004 (2010).

[75] F. Gross and S. Liuti, Phys. Rev. C **45**, 1374 (1992).

[76] W. Melnitchouk, A. W. Schreiber and A. W. Thomas, Phys. Lett. B **335**, 11 (1994).

[77] W. Melnitchouk, M. Sargsian and M. I. Strikman, Z. Phys. A **359**, 99 (1997).

[78] D. W. Marquardt, J. Soc. Ind. Appl. Math. **11**, 431 (1963).

[79] P. R. Bevington, "Data Reduction and Error Analysis for the Physical Sciences" (McGraw-Hill, 1969).

[80] J. Pumplin *et al.*, JHEP **0207**, 012 (2003).

[81] A. D. Martin, R. G. Roberts, W. J. Stirling and R. S. Thorne, Eur. Phys. J. C **28**, 455 (2003).

[82] The CTEQ collaboration website, `http://www.cteq.org`.

[83] A. D. Martin, A. J. Th. M. Mathijssen, W. J. Stirling, R. S. Thorne, B. J. A. Watt and G. Watt, arXiv:1211.1215 [hep-ph].

[84] A. Accardi, AIP Conf. Proc. **1369**, 210 (2011).

[85] D. Stump *et al.*, JHEP **0310**, 046 (2003).

[86] J. Anderson [LHCb Collaboration], arXiv:1109.3371 [hep-ex].

[87] D. d'Enterria and J. Rojo, Nucl. Phys. **B860**, 311 (2012), arXiv:1202.1762[hep-ph].

[88] Y. Liang *et al.* [Jefferson Lab Hall C E94-110 Collaboration], arXiv:nucl-ex/0410027.

[89] P. Monaghan, A. Accardi, M. E. Christy, C. E. Keppel, W. Melnitchouk and L. Zhu, arXiv:1209.4542 [nucl-ex].

[90] S. J. Brodsky, F. Fleuret, C. Hadjidakis and J. P. Lansberg, Phys. Rept. (2012) in press, `http://dx.doi.org/10.1016/j.physrep.2012.10.001`.

[91] Jefferson Lab Experiment C12-10-103 [MARATHON], G. G. Petratos, J. Gomez, R. J. Holt and R. D. Ransome, spokespersons.

[92] Jefferson Lab Experiment E12-10-102 [BONUS12], S. Bültmann, M. E. Christy, H. Fenker, K. Griffioen, C. E. Keppel, S. Kuhn and W. Melnitchouk, spokespersons.

[93] Jefferson Lab Experiment E12-10-007 [SoLID], P. Souder, spokesperson.